Science Advances
AAAS

Supplementary Materials for

Microfluidic bioprinting of tough hydrogel-based vascular conduits for functional blood vessels

Di Wang *et al.*

Corresponding author: Yu Shrike Zhang, yszhang@research.bwh.harvard.edu; Xuanhe Zhao, zhaox@mit.edu; C. Keith Ozaki, ckozaki1@bwh.harvard.edu

Sci. Adv. **8**, eabq6900 (2022)
DOI: 10.1126/sciadv.abq6900

The PDF file includes:

Figs. S1 to S16
Table S1
Legends for movies S1 to S6
References

Other Supplementary Material for this manuscript includes the following:

Movies S1 to S6

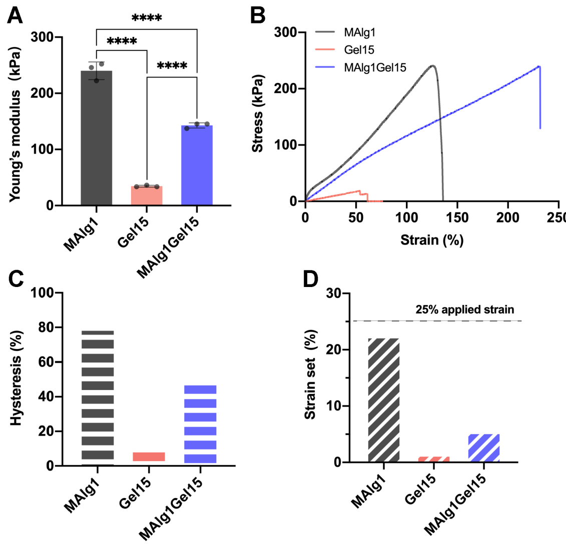

Fig. S1. Effect of components on DN hydrogel mechanical properties. **(A)** Young's moduli, **(B)** Uniaxial tensile stress–strain curves, **(C)** hysteresis ratios, and **(D)** strain sets after applying a maximum strain of 25% for MAlg1, Gel15, and MAlg1Gel15. ****$p < 0.0001$.

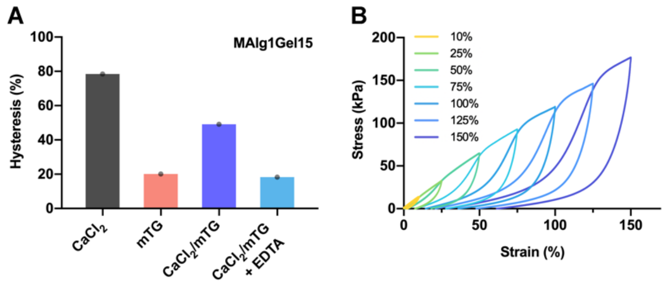

Fig. S2. Effect of curing conditions on DN hydrogel mechanical properties. **(A)** Hysteresis ratio of hybrid hydrogel (MAlg1Gel15) with different curing conditions and post-treatment. **(B)** Successive loading–unloading stress–strain curves of MAlg1Gel15 DN hydrogel with different maximum applied strains from 10% to 150%.

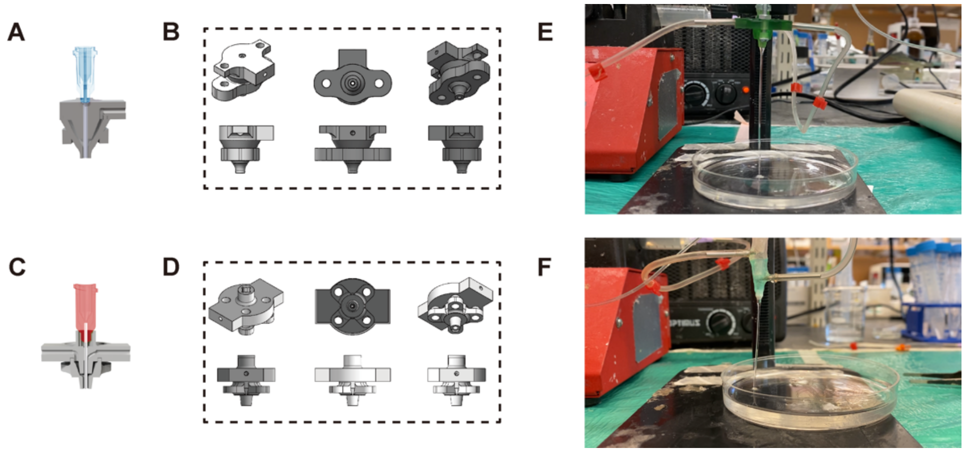

Fig. S3. Two types of multichannel coaxial extrusion systems. **(A)** General view of the two-channel nozzle for (bio)printing of mono-layered tubes. **(B)** Additional views of the two-channel nozzle. **(C)** General view of three-channel nozzle for (bio)printing of dual-layered tubes. **(D)** Additional views of the three-channel nozzle. Vascular conduit printing using (**E**) a coaxial extrusion nozzle assembled assisted by the 3D-printed BNS, and (**F**) a coaxial extrusion nozzle made entirely from commercial needles.

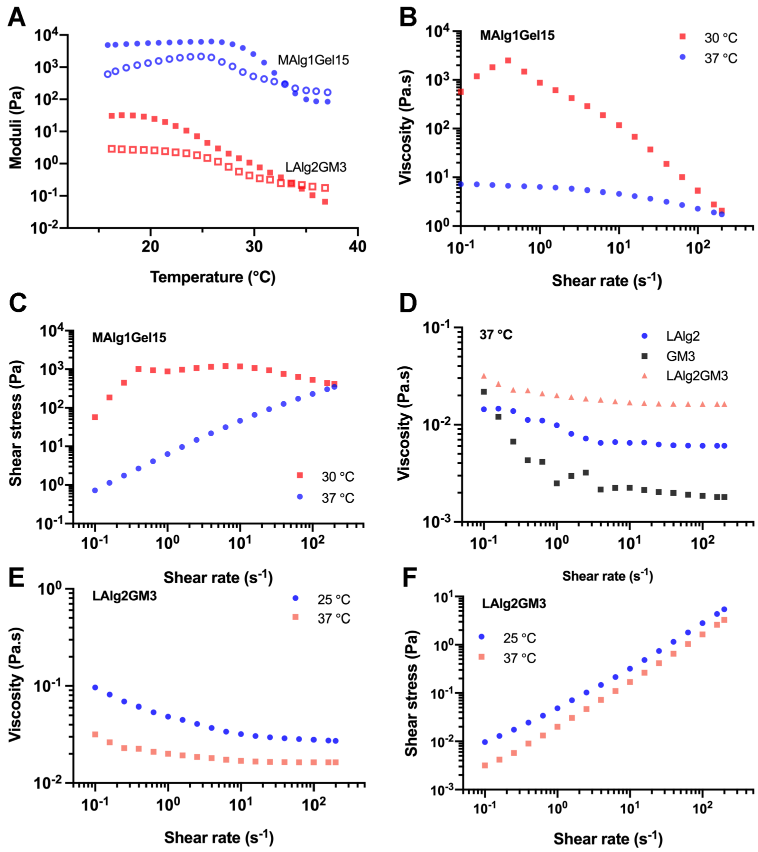

Fig. S4. Rheological measurements of the two hybrid (bio)inks. **(A)** Storage moduli (solid marks) and loss moduli (open marks) as a function of temperature for the two different (bio)inks. **(B)** Apparent viscosities and **(C)** shear stresses of the hybrid (bio)ink MAlg1Gel15 as a function of shear rate at 30 and 37 ºC measured by flow-sweep. **(D)** Apparent viscosities of LAlg2, GM3, and LAlg2GM3 as a function of shear rate at 37 ºC. **(E)** Apparent viscosities and **(F)** shear stresses of the hybrid (bio)ink of LAlg2GM3 as a function of shear rate at 25 and 37 ºC measured by flow-sweep.

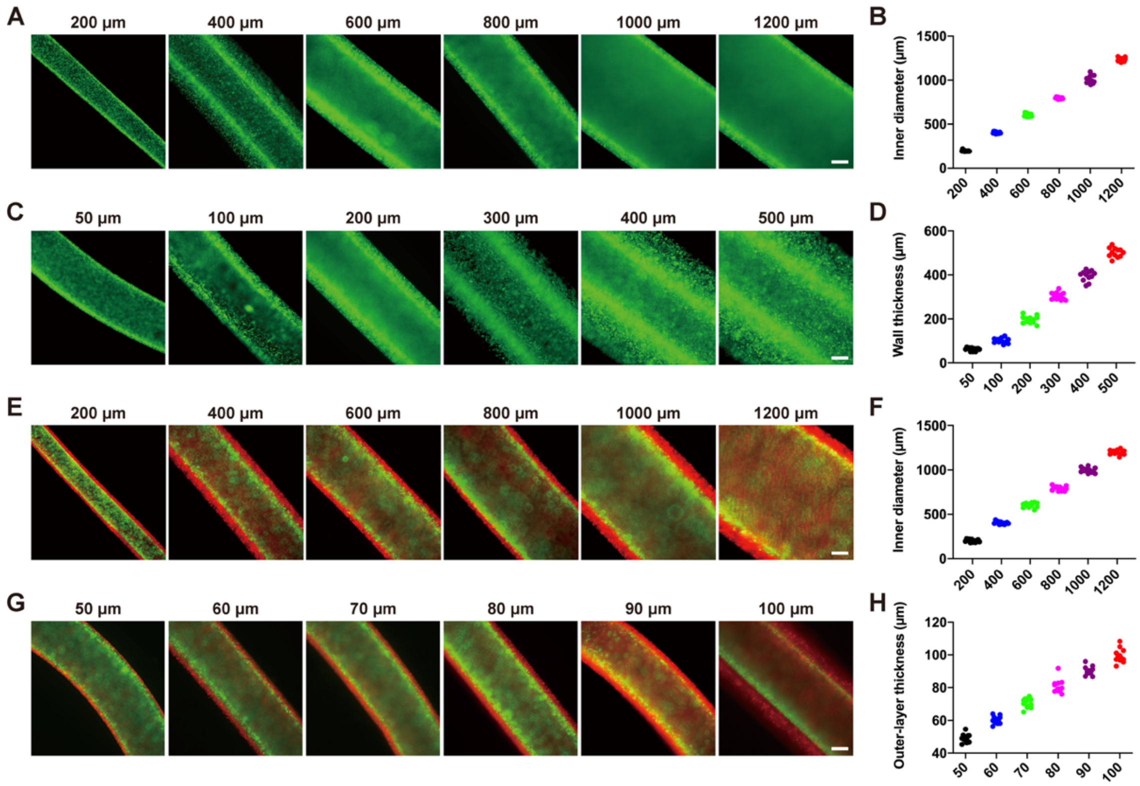

Fig. S5. Demonstration of (bio)printed size-tunable vascular acellular conduits. **(A)** Diameter-tunable mono-layered conduits. **(B)** Inner diameter of mono-layered conduits. **(C)** Wall thickness-tunable mono-layered conduits. **(D)** Wall thickness of mono-layered conduits. **(E)** Diameter-tunable dual-layered conduits. **(F)** Inner diameter of dual-layered conduits. **(G)** Wall thickness-tunable dual-layered conduits. **(H)** Outer-layer thickness of dual-layered conduits. Scale bars, 200 µm.

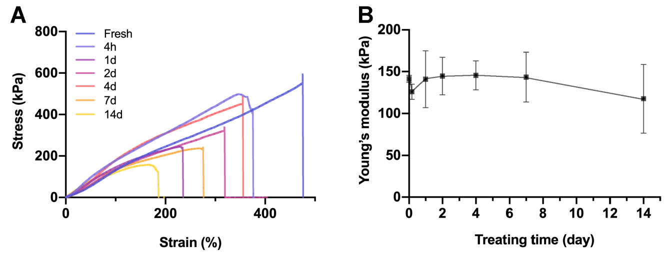

Fig. S6. Mechanical properties of (bio)printed MAlgGel15 tubes after treatment with SMC culture medium at 37 ºC. **(A)** Tensile stress–strain curves and **(B)** Young's moduli of (bio)printed tubes after treatment in SMC culture medium for different times.

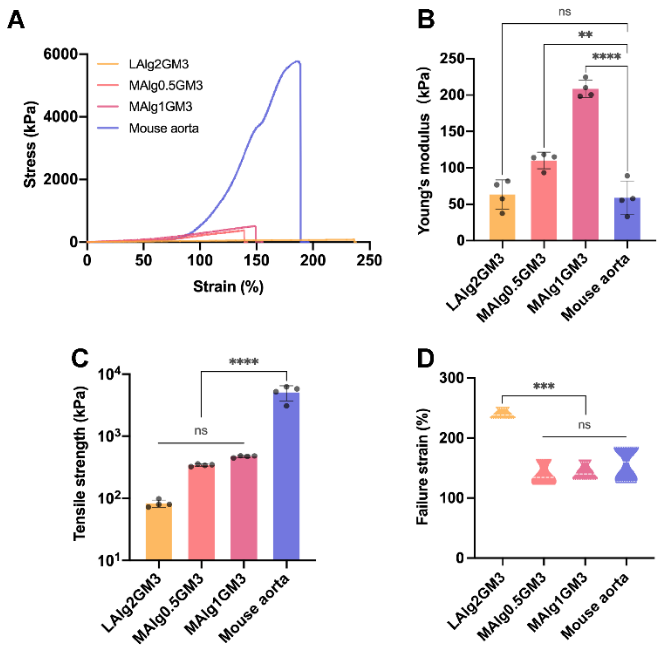

Fig. S7. Comparisons of mechanical properties of the (bio)printed dual-layered vascular tubes with different (bio)inks and the mouse aorta: **(A)** tensile stress–strain curves, **(B)** Young's moduli, **(C)** tensile strengths, and **(D)** failure strains. ns: no significant difference, $^{**}p < 0.01$, $^{***}p < 0.001$, $^{****}p < 0.0001$.

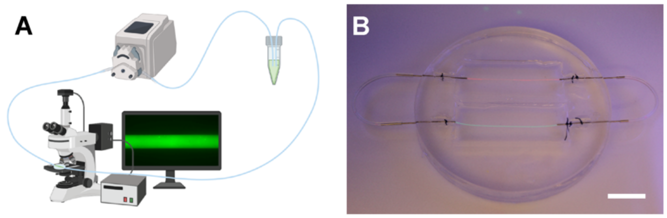

Fig. S8. The circulation and bioreactor setup for diffusion tests. **(A)** Schematic of the circulation system including a peristaltic pump connected to a tube containing FITC-Dex solution perfused through the chip-fitted vascular conduit, observed under a microscope. **(B)** Photograph of a two-channel bioreactor with two (bio)printed conduits connected. Scale bar, 2 cm.

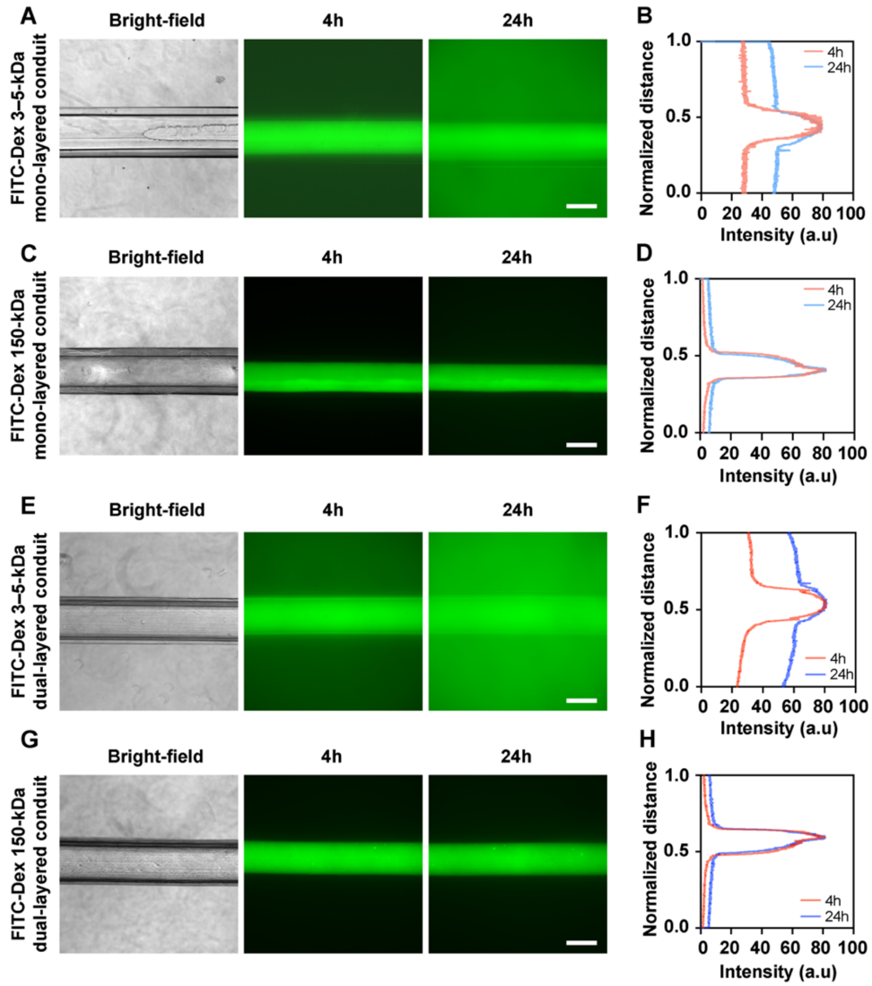

Fig. S9. Diffusion and permeability measurements of (bio)printed mono-layered and dual-layered conduits. **(A, C)** Bright-field and fluorescence images and **(B, D)** fluorescence intensity profiles of 3–5-kDa and 150-kDa FITC-Dex permeability tests in mono-layered conduits. **(E, G)** Bright-field and fluorescence images and **(F, H)** fluorescence intensity profiles of 3–5-kDa and 150-kDa FITC-Dex permeability tests in dual-layered conduits. Scale bars, 500 μm.

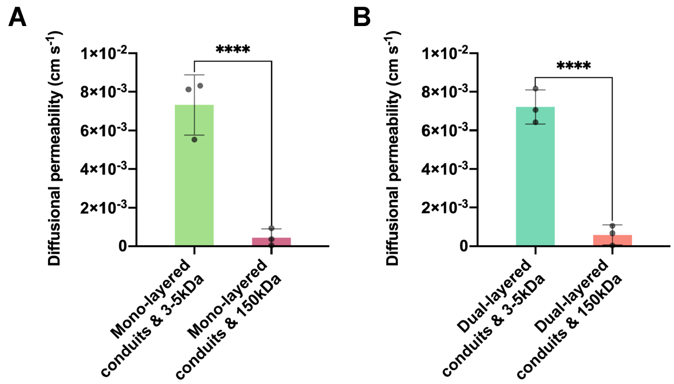

Fig. S10. Quantified diffusional permeability of small- and large-M_w fluorescence molecules. Diffusional permeability values in **(A)** mono-layered conduits and **(B)** dual-layered conduits. ****$p < 0.0001$.

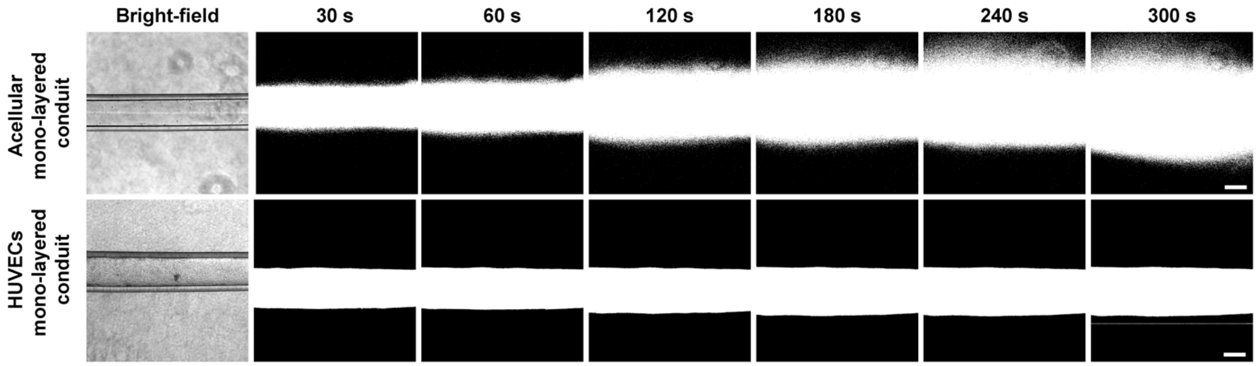

Fig. S11. Diffusion profiles of 3–5-kDa FITC-Dex from (bio)printed mono-layered conduits with and without HUVEC layer in the lumen at selected time points. Scale bars, 200 μm.

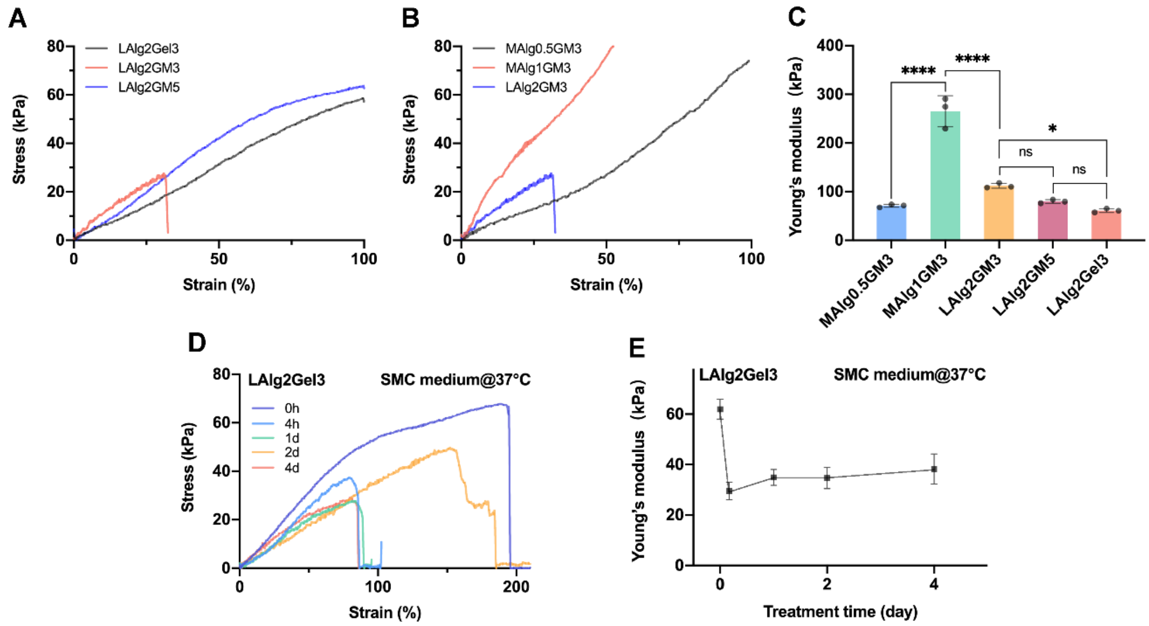

Fig. S12. Mechanical properties of (bio)printed acellular mono-layered tubes featuring different outer-layer (bio)inks. Tensile stress–strain curves of **(A)** (bio)printed tubes consisting of 2% low-viscosity alginate and different contents of GelMA or gelatin, and **(B)** (bio)printed tubes consisting of 3% GelMA and different types and contents of alginate. **(C)** Young's moduli of all the samples in (A) and (B). **(D)** Tensile stress–strain curves and **(E)** Young's modulus variations of (bio)printed LAlg2Gel3 tubes immersed in SMC medium at 37 °C for indicated times. ns: no significant difference, $^{*}p < 0.05$, $^{****}p < 0.0001$.

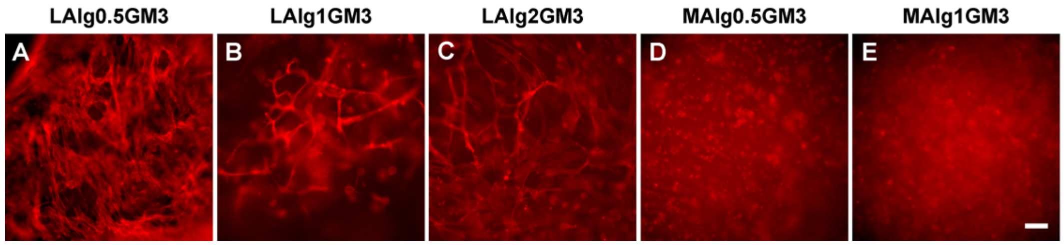

Fig. S13. F-actin staining of encapsulated HUASMCs in different bioinks at day 7. **(A)** LAlg0.5GM3, **(B)** LAlg1GM3, **(C)** LAlg2GM3, **(D)** MAlg0.5GM3, and **(E)** MAlg1GM3 bioinks. Scale bars, 100 μm.

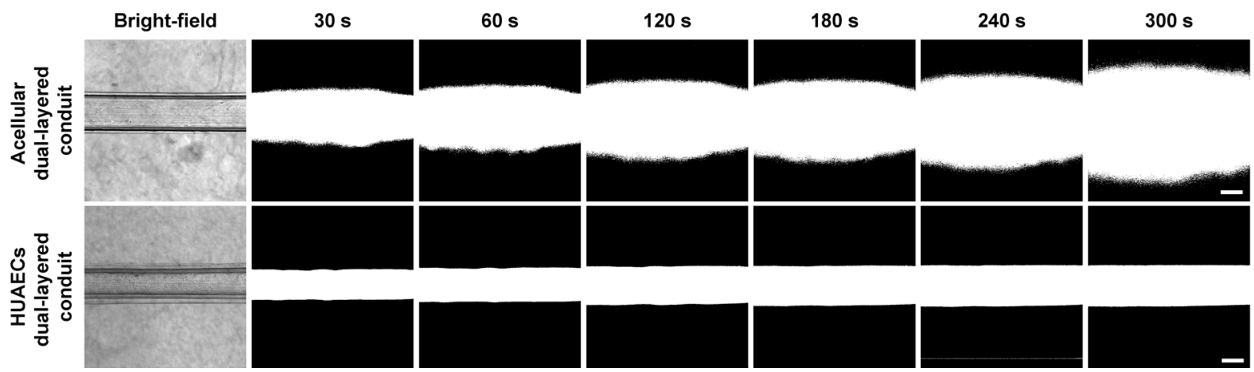

Fig. S14. Diffusion profiles of 3–5-kDa FITC-Dex across the walls of the (bio)printed dual-layered conduits in the absence (top) and the presence (bottom) of HUAEC layer in the lumen at selected time points. Scale bars, 200 μm.

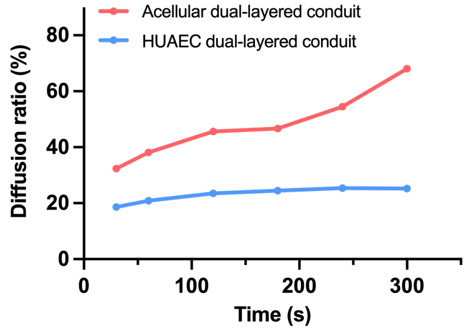

Fig. S15. Quantified diffusion ratios of 3–5-kDa FITC-Dex as a function of time in the absence and presence of HUAEC layer in the lumen of dual-layered conduits.

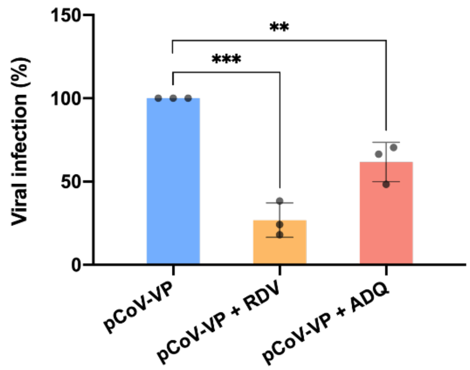

Fig. S16. Quantified infections of the venous conduits with pCoV-VPs. **$p < 0.01$, ***$p < 0.001$.

Table S1. Comparisons of mechanical and biological performances for (bio)printed vascular conduits.

Materials	Young's Modulus (kPa)	Ultimate Tensile Strength (kPa)	Failure Strain (%)	Burst Pressure (mmHg)	Perfusability	Barrier Performance	Vasoactivity	Biomarker Expressions	Applications	Study*
Alginate	105–341	110–382	69–82	43–303	Yes	Yes	-	-	-	Zhang 2015 (*29*)
Alginate	-	46–116	155–96	-	Yes	Yes	-	-	-	Gao 2015 (*70*)
GelMA, alginate, PEGTA	24–51	-	-	-	Yes	-	-	CD31, *α*-SMA	-	Jia 2016 (*26*)
VdECM, alginate, PLGA microspheres	-	-	-	-	Yes	-	-	CD31, *α*-SMA	*In vivo* grafts, *in vitro* models	Gao 2017 (*71*)
VdECM, alginate	-	-	-	-	Yes	Yes	-	CD31, VE-cadherin, laminin	*In vitro* models	Gao 2018 (*24*)
GelMA, alginate, PEGOA	≈12	-	-	-	Yes	-	-	ZO-1, VE-cadherin, *α*-SMA, VE-cadherin	-	Pi 2018 (*27*)
VdECM, alginate	-	47–195	-	63–174	Yes	-	Contraction	Elastin, R-COL-1, H-COL-1, H-*α*-SMA, CD31	*In vivo* grafts	Gao 2019 (*72*)
Gelatin, PEG, tyramine	-	-	-	-	-	-	-	-	-	Hong 2019 (*22*)
Alginate	-	-	-	-	Yes	Yes	Contraction	*α*-SMA, CD31, Laminin, Tubulin	-	Andrique 2019 (*23*)
F127, BUM	-	-	-	-	Yes	-	-	CD31	-	Millik 2019 (73)
VdECM, alginate	-	-	-	-	Yes	Yes	-	*α*-SMA, CD31, H-COL-1	*In vitro* models	Gao 2021 (*25*)
GelMA, nanoclay, NAGA	≈21,000	≈22,000	≈500	≈2,500	Yes	Yes	-	CD31, vWF	-	Liang 2020 (*28*)
GelMA, gelatin	1–6	-	-	-	-	-	-	CD31	*In vitro* models	Shao 2020 (74)
Alginate, gelatin (or GelMA)	171 (mono-layered), 63 (dual-layered)	538 (mono-layered), 82 (dual-layered)	184 (mono-layered), 240 (dual-layered)	1,113–1,498 (mono-layered), 1,138 (dual-layered)	Yes	Yes	Contraction, Dilation	ZO-1, VE-cadherin, Laminin, Tubulin, ACE-2, *α*-1a adrenergic, acetylcholine	*In vivo* grafts, *in vitro* models	This study

Movie S1. Tensile tests applied on **(A)** a (bio)printed mono-layered conduit and **(B)** a mouse *vena cava*. Replayed at 16× speed.

Movie S2. Burst pressure tests for **(A)** a (bio)printed vascular conduits, **(B)** a mouse *vena cava*, and **(C)** a mouse aorta. Replayed at 1× speed.

Movie S3. Perfusion of RBC suspension into a (bio)printed long mono-layered conduit. Replayed at 1× speed.

Movie S4. Demonstration of a bioreactor for permeability experiments. Replayed at 8× speed.

Movie S5. Permeability tests applied on (bio)printed vascular conduits in the presence or absence of endothelial cells within the first 10 min. **(A)** an acellular mono-layered conduit, **(B)** a mono-layered conduit with confluent HUVECs in the lumen, **(C)** an acellular dual-layered conduit, **(D)** a dual-layered conduit with confluent HUAECs in the lumen. Replayed at 8× speed.

Movie S6. Anastomose tests of (bio)printed vascular conduits and native blood vessels by perfusing fluorescent beads. **(A)** a small-sized (bio)printed vascular conduit anastomosed with a mouse aorta on a 3-cm petri dish, **(B)** a large-size (bio)printed vascular conduit anastomosed with a human popliteal vein on a 10-cm petri dish. Replayed at 1× speed.

REFERENCES AND NOTES

1. C. Hwa, A. Sebastian, W. C. Aird, Endothelial biomedicine: Its status as an interdisciplinary field, its progress as a basic science, and its translational bench-to-bedside gap. *Endothelium* **12**, 139–151 (2005).

2. S. P. Herbert, D. Y. R. Stainier, Molecular control of endothelial cell behaviour during blood vessel morphogenesis. *Nat. Rev. Mol. Cell Biol.* **12**, 551–564 (2011).

3. W. D. Tucker, Y. Arora, K. Mahajan, *Anatomy, Blood Vessels* (StatPearls Publishing LLC., 2021).

4. S. S. Virani, A. Alonso, H. J. Aparicio, E. J. Benjamin, M. S. Bittencourt, C. W. Callaway, A. P. Carson, A. M. Chamberlain, S. Cheng, F. N. Delling, M. S. V. Elkind, K. R. Evenson, J. F. Ferguson, D. K. Gupta, S. S. Khan, B. M. Kissela, K. L. Knutson, C. D. Lee, T. T. Lewis, J. Liu, M. S. Loop, P. L. Lutsey, J. Ma, J. Mackey, S. S. Martin, D. B. Matchar, M. E. Mussolino, S. D. Navaneethan, A. M. Perak, G. A. Roth, Z. Samad, G. M. Satou, E. B. Schroeder, S. H. Shah, C. M. Shay, A. Stokes, L. B. VanWagner, N. Y. Wang, C. W. Tsao; American Heart Association Council on Epidemiology and Prevention Statistics Committee and Stroke Statistics Subcommittee, Heart disease and stroke statistics-2021 update: A report from the american heart association. *Circulation* **143**, e254–e743 (2021).

5. G. A. Roth, G. A. Mensah, C. O. Johnson, G. Addolorato, E. Ammirati, L. M. Baddour, N. C. Barengo, A. Z. Beaton, E. J. Benjamin, C. P. Benziger, A. Bonny, M. Brauer, M. Brodmann, T. J. Cahill, J. Carapetis, A. L. Catapano, S. S. Chugh, L. T. Cooper, J. Coresh, M. Criqui, N. DeCleene, K. A. Eagle, S. Emmons-Bell, V. L. Feigin, J. Fernández-Solà, G. Fowkes, E. Gakidou, S. M. Grundy, F. J. He, G. Howard, F. Hu, L. Inker, G. Karthikeyan, N. Kassebaum, W. Koroshetz, C. Lavie, D. Lloyd-Jones, H. S. Lu, A. Mirijello, A. M. Temesgen, A. Mokdad, A. E. Moran, P. Muntner, J. Narula, B. Neal, M. Ntsekhe, G. Moraes de Oliveira, C. Otto, M. Owolabi, M. Pratt, S. Rajagopalan, M. Reitsma, A. L. P. Ribeiro, N. Rigotti, A. Rodgers, C. Sable, S. Shakil, K. Sliwa-Hahnle, B. Stark, J. Sundström, P. Timpel, I. M. Tleyjeh, M. Valgimigli, T. Vos, P. K. Whelton, M. Yacoub, L. Zuhlke, C. Murray, V. Fuster, Global Burden of Cardiovascular Diseases and Risk Factors, Global burden of cardiovascular diseases and risk factors, 1990–2019. *J. Am. Coll. Cardiol.* **76**, 2982–3021 (2020).

6. L. D. Hillis, P. K. Smith, J. L. Anderson, J. A. Bittl, C. R. Bridges, J. G. Byrne, J. E. Cigarroa, V. J. DiSesa, L. F. Hiratzka, A. M. Hutter, Jr., M. E. Jessen, E. C. Keeley, S. J. Lahey, R. A. Lange, M. J. London, M. J. Mack, M. R. Patel, J. D. Puskas, J. F. Sabik, O. Selnes, D. M. Shahian, J. C. Trost, M. D. Winniford, A. K. Jacobs, J. L. Anderson, N. Albert, M. A. Creager, S. M. Ettinger, R. A. Guyton, J. L. Halperin, J. S. Hochman, F. G. Kushner, E. M. Ohman, W. Stevenson, C. W. Yancy; American College of Cardiology Foundation/American Heart Association Task Force on Practice Guidelines, 2011 ACCF/AHA guideline for coronary artery bypass graft surgery: Executive summary: A report of the American College of Cardiology Foundation/American Heart Association Task Force on practice guidelines. *J. Thorac. Cardiovasc. Surg.* **143**, 4–34 (2012).

7. I. Ahmed, S. Yandrapalli, *Internal Mammary Artery Bypass* (StatPearls Publishing LLC., 2021).

8. P. Altshuler, P. Nahirniak, N. J. Welle, *Saphenous Vein Grafts* (StatPearls Publishing LLC., 2021).

9. STS data clarifies variables behind coronary artery bypass complication, mortality rates. *Data Strateg. Benchmarks* **2**, 172–174, 161 (1998).

10. A. L. Hawkes, M. Nowak, B. Bidstrup, R. Speare, Outcomes of coronary artery bypass graft surgery. *Vasc. Health Risk Manag.* **2**, 477–484 (2006).

11. B. McNichols, J. R. Spratt, J. George, S. Rizzi, E. W. Manning, K. Park, Coronary artery bypass: Review of surgical techniques and impact on long-term revascularization outcomes. *Cardiol. Ther.* **10**, 89–109 (2021).

12. J. G. Motwani, E. J. Topol, Aortocoronary saphenous vein graft disease. *Circulation* **97**, 916–931 (1998).

13. A. Malinska, Z. Podemska, B. Perek, M. Jemielity, P. Buczkowski, M. Grzymislawska, P. Sujka-Kordowska, M. Nowicki, Preoperative factors predicting saphenous vein graft occlusion in coronary artery bypass grafting: A multivariate analysis. *Histochem. Cell Biol.* **148**, 417–424 (2017).

14. A. Lejay, V. Vento, S. Kuntz, L. Steinmetz, Y. Georg, F. Thaveau, F. Heim, N. Chakfé, Current status on vascular substitutes. *J. Cardiovasc. Surg. (Torino)* **61**, 538–543 (2020).

15. H.-H. Greco Song, R. T. Rumma, C. K. Ozaki, E. R. Edelman, C. S. Chen, Vascular tissue engineering: Progress, challenges, and clinical promise. *Cell Stem Cell* **22**, 340–354 (2018).

16. M. D. Sarker, S. Naghieh, N. K. Sharma, L. Ning, X. Chen, Bioprinting of vascularized tissue scaffolds: Influence of biopolymer, cells, growth factors, and gene delivery. *J. Healthc. Eng.* **2019**, 9156921 (2019).

17. X. Cao, S. Maharjan, R. Ashfaq, J. Shin, Y. S. Zhang, Bioprinting of small-diameter blood vessels. *Engineering* **7**, 832–844 (2021).

18. P. Sasmal, P. Datta, Y. Wu, I. T. Ozbolat, 3D bioprinting for modelling vasculature. *Microphysiol. Syst.* **2**, 9 (2018).

19. Y. S. Zhang, G. Haghiashtiani, T. Hübscher, D. J. Kelly, J. M. Lee, M. Lutolf, M. C. McAlpine, W. Y. Yeong, M. Zenobi-Wong, J. Malda, 3D extrusion bioprinting. *Nat. Rev. Methods Primers* **1**, 75 (2021).

20. D. N. d. Chatinier, K. P. Figler, P. Agrawal, W. Liu, Y. S. Zhang, The potential of microfluidics-enhanced extrusion bioprinting. *Biomicrofluidics* **15**, 041304 (2021).

21. M. Costantini, C. Colosi, W. Święszkowski, A. Barbetta, Co-axial wet-spinning in 3D bioprinting: State of the art and future perspective of microfluidic integration. *Biofabrication* **11**, 012001 (2019).

22. S. Hong, S. K. Ji, B. Jung, C. Won, C. Hwang, Coaxial bioprinting of cell-laden vascular constructs using a gelatin-tyramine bioink. *Biomater. Sci.* **7**, 4578–4587 (2019).

23. L. Andrique, G. Recher, K. Alessandri, N. Pujol, M. Feyeux, P. Bon, L. Cognet, P. Nassoy, A. Bikfalvi, A model of guided cell self-organization for rapid and spontaneous formation of functional vessels. *Sci. Adv.* **5**, eaau6562 (2019).

24. G. Gao, J. Y. Park, B. S. Kim, J. Jang, D.-W. Cho, Coaxial cell printing of freestanding, perfusable, and functional in vitro vascular models for recapitulation of native vascular endothelium pathophysiology. *Adv. Healthc. Mater.* **7**, 1801102 (2018).

25. G. Gao, W. Park, B. S. Kim, M. Ahn, S. Chae, W.-W. Cho, J. Kim, J. Y. Lee, J. Jang, D.-W. Cho, Construction of a novel in vitro atherosclerotic model from geometry-tunable artery equivalents engineered via in-bath coaxial cell printing. *Adv. Funct. Mater.* **31**, 2008878 (2021).

26. W. Jia, P Selcan Gungor-Ozkerim, Y. S. Zhang, K. Yue, K. Zhu, W. Liu, Q. Pi, B. Byambaa, M. R. Dokmeci, S. R. Shin, A. Khademhosseini, Direct 3D bioprinting of perfusable vascular constructs using a blend bioink. *Biomaterials* **106**, 58–68 (2016).

27. Q. Pi, S. Maharjan, X. Yan, X. Liu, B. Singh, A. M. van Genderen, F. Robledo-Padilla, R. Parra-Saldivar, N. Hu, W. Jia, C. Xu, J. Kang, S. Hassan, H. Cheng, X. Hou, A. Khademhosseini, Y. S. Zhang, Digitally tunable microfluidic bioprinting of multilayered cannular tissues. *Adv. Mat.* **30**, e1706913 (2018).

28. Q. Liang, F. Gao, Z. Zeng, J. Yang, M. Wu, C. Gao, D. Cheng, H. Pan, W. Liu, C. Ruan, Coaxial scale-up printing of diameter-tunable biohybrid hydrogel microtubes with high strength, perfusability, and endothelialization. *Adv. Funct. Mater.* **30**, 2001485 (2020).

29. Y. Zhang, Y. Yu, A. Akkouch, A. Dababneh, F. Dolati, I. T. Ozbolat, In vitro study of directly bioprinted perfusable vasculature conduits. *Biomater. Sci.* **3**, 134–143 (2015).

30. J. P. Gong, Y. Katsuyama, T. Kurokawa, Y. Osada, Double-network hydrogels with extremely high mechanical strength. *Adv. Mat.* **15**, 1155–1158 (2003).

31. X. Zhao, X. Chen, H. Yuk, S. Lin, X. Liu, G. Parada, Soft materials by design: Unconventional polymer networks give extreme properties. *Chem. Rev.* **121**, 4309–4372 (2021).

32. N. Contessi Negrini, A. Angelova Volponi, P. T. Sharpe, A. D. Celiz, Tunable cross-linking and adhesion of gelatin hydrogels via bioorthogonal click chemistry. *ACS Biomater Sci. Eng.* **7**, 4330–4346 (2021).

33. C. W. Yung, L. Q. Wu, J. A. Tullman, G. F. Payne, W. E. Bentley, T. A. Barbari, Transglutaminase crosslinked gelatin as a tissue engineering scaffold. *J. Biomed. Mater. Res. A* **83**, 1039–1046 (2007).

34. J. P. Gong, Why are double network hydrogels so tough? *Soft Matter* **6**, 2583–2590 (2010).

35. O. Chaudhuri, L. Gu, D. Klumpers, M. Darnell, S. A. Bencherif, J. C. Weaver, N. Huebsch, H.-p. Lee, E. Lippens, G. N. Duda, D. J. Mooney, Hydrogels with tunable stress relaxation regulate stem cell fate and activity. *Nat. Mater.* **15**, 326–334 (2016).

36. J. Li, Y. Wu, J. He, Y. Huang, A new insight to the effect of calcium concentration on gelation process and physical properties of alginate films. *J. Mater. Sci.* **51**, 5791–5801 (2016).

37. B. G. Compton, J. A. Lewis, 3D-printing of lightweight cellular composites. *Adv. Mat.* **26**, 5930–5935 (2014).

38. S. A. Ghodbane, N. S. Murthy, M. G. Dunn, J. Kohn, Achieving molecular orientation in thermally extruded 3D printed objects. *Biofabrication* **11**, 045004 (2019).

39. J. L. Drury, R. G. Dennis, D. J. Mooney, The tensile properties of alginate hydrogels. *Biomaterials* **25**, 3187–3199 (2004).

40. S. K. Burke, K. Bingham, E. Moss, D. P. Gottlieb, M. D. Wong, K. S. Bland, F. N. Franano, Recombinant human elastase alters the compliance of atherosclerotic tibial arteries after ex vivo angioplasty. *J. Cardiovasc. Pharmacol.* **67**, 305–311 (2016).

41. J. Gavard, Endothelial permeability and VE-cadherin: A wacky comradeship. *Cell Adh. Migr.* **7**, 455–461 (2013).

42. W. Liu, Z. Zhong, N. Hu, Y. Zhou, L. Maggio, A. K. Miri, A. Fragasso, X. Jin, A. Khademhosseini, Y. S. Zhang, Coaxial extrusion bioprinting of 3D microfibrous constructs with cell-favorable gelatin methacryloyl microenvironments. *Biofabrication* **10**, 024102 (2018).

43. S. Pashneh-Tala, S. MacNeil, F. Claeyssens, The tissue-engineered vascular graft-past, present, and future. *Tissue Eng. Part B Rev.* **22**, 68–100 (2016).

44. "Structure and function of blood vessels"; https://courses.lumenlearning.com/suny-ap2/chapter/structure-and-function-of-blood-vessels/.

45. A. Banerjee, M. Arha, S. Choudhary, R. S. Ashton, S. R. Bhatia, D. V. Schaffer, R. S. Kane, The influence of hydrogel modulus on the proliferation and differentiation of encapsulated neural stem cells. *Biomaterials* **30**, 4695–4699 (2009).

46. M. J. Davis, M. A. Hill, Signaling mechanisms underlying the vascular myogenic response. *Physiol. Rev.* **79**, 387–423 , (1999).

47. M. A. Hill, G. A. Meininger, M. J. Davis, I. Laher, Therapeutic potential of pharmacologically targeting arteriolar myogenic tone. *Trends Pharmacol. Sci.* **30**, 363–374 (2009).

48. K. F. Franzen, M. Meusel, J. Engel, T. Röcker, D. Drömann, F. Sayk, Differential effects of Angiotensin-II compared to phenylephrine on arterial stiffness and hemodynamics: A placebo-controlled study in healthy humans. *Cells* **10**, 1108 (2021).

49. H. B. Nguyen, S. Y. Lee, S. H. Park, M. Y. Lee, I. H. Chang, S. C. Myung, Relaxing effect of acetylcholine on phenylephrine-induced contraction of isolated rabbit prostate strips is mediated by neuronal nitric oxide synthase. *Korean J. Urol.* **54**, 333–338 (2013).

50. "COVID-19 dashboard by the Center for Systems Science and Engineering (CSSE) at Johns Hopkins University (JHU)"; https://coronavirus.jhu.edu/map.html.

51. C. B. Jackson, M. Farzan, B. Chen, H. Choe, Mechanisms of SARS-CoV-2 entry into cells. *Nat. Rev. Mol. Cell Biol.* **23**, 3–20 (2022).

52. K. Katella, "Omicron, delta, alpha, and more: What to know about the coronavirus variants" (Yale Medicine, 2022); www.yalemedicine.org/news/covid-19-variants-of-concern-omicron.

53. S. K. Abrokwa, S. A. Müller, A. Méndez-Brito, J. Hanefeld, C. El Bcheraoui, Recurrent SARS-CoV-2 infections and their potential risk to public health - A systematic review. *PLOS ONE* **16**, e0261221 (2021).

54. R. Rauti, M. Shahoha, Y. Leichtmann-Bardoogo, R. Nasser, E. Paz, R. Tamir, V. Miller, T. Babich, K. Shaked, A. Ehrlich, K. Ioannidis, Y. Nahmias, R. Sharan, U. Ashery, B. M. Maoz, Effect of SARS-CoV-2 proteins on vascular permeability. *eLife* **10**, e69314 (2021).

55. L. C. Barbosa, T. L. Gonçalves, L. Prudencio de Araujo, L. Vieira de Oliveira Rosario, V. P. Ferrer, Endothelial cells and SARS-CoV-2: An intimate relationship. *Vascul. Pharmacol.* **137**, 106829 (2021).

56. COVID-19 and vascular disease. *EBioMedicine* **58**, 102966 (2020).

57. A. J. Pruijssers, A. S. George, A. Schäfer, S. R. Leist, L. E. Gralinksi, K. H Dinnon III, B. L. Yount, M. L. Agostini, L. J. Stevens, J. D. Chappell, X. Lu, T. M. Hughes, K. Gully, D. R. Martinez, A. J. Brown, R. L. Graham, J. K. Perry, V. D. Pont, J. Pitts, B. Ma, D. Babusis, E. Murakami, J. Y. Feng, J. P. Bilello, D. P. Porter, T. Cihlar, R. S. Baric, M. R. Denison, T. P. Sheahan, Remdesivir inhibits SARS-CoV-2 in human lung cells and chimeric SARS-CoV expressing the SARS-CoV-2 RNA polymerase in mice. *Cell Rep.* **32**, 107940 (2020).

58. S. Weston, C. M. Coleman, R. Haupt, J. Logue, M. B. Frieman, Broad anti-coronavirus activity of Food and Drug Administration-approved drugs against SARS-CoV-2 *in vitro* and SARS-CoV *in vivo*. *J. Virol.* **94**, e01218–e01220 (2020).

59. C. L. Onweni, Y. S. Zhang, T. Caulfield, C. E. Hopkins, D. L. Fairweather, W. D. Freeman, ACEI/ARB therapy in COVID-19: The double-edged sword of ACE2 and SARS-CoV-2 viral docking. *Crit. Care* **24**, 475 (2020).

60. A. G. Harrison, T. Lin, P. Wang, Mechanisms of SARS-CoV-2 transmission and pathogenesis. *Trends Immunol.* **41**, 1100–1115 (2020).

61. J. Gong, C. C. L. Schuurmans, A. M. van Genderen, X. Cao, W. Li, F. Cheng, J. J. He, A. López, V. Huerta, J. Manríquez, R. Li, H. Li, C. Delavaux, S. Sebastian, P. E. Capendale, H. Wang, J. Xie, M. Yu, R. Masereeuw, T. Vermonden, Y. S. Zhang, Complexation-induced resolution enhancement of 3D-printed hydrogel constructs. *Nat. Commun.* **11**, 1267 (2020).

62. S. Maharjan, J. Alva, C. Cámara, A. G. Rubio, D. Hernández, C. Delavaux, E. Correa, M. D. Romo, D. Bonilla, M. L. Santiago, W. Li, F. Cheng, G. Ying, Y. S. Zhang, Symbiotic photosynthetic oxygenation within 3D-bioprinted vascularized tissues. *Matter* **4**, 217–240 (2021).

63. H. Ravanbakhsh, Z. Luo, X. Zhang, S. Maharjan, H. S. Mirkarimi, G. Tang, C. Chávez-Madero, L. Mongeau, Y. S. Zhang, Freeform cell-laden cryobioprinting for shelf-ready tissue fabrication and storage. *Matter* **5**, 573–593 (2022).

64. H. Han, Y. Park, Y.-M. Choi, U. Yong, B. Kang, W. Shin, S. Min, H. J. Kim, J. Jang, A bioprinted tubular intestine model using a colon-specific extracellular matrix bioink. *Adv. Healthc. Mater.* **11**, 2101768 (2022).

65. C. Xiang, Z. Wang, C. Yang, X. Yao, Y. Wang, Z. Suo, Stretchable and fatigue-resistant materials. *Mater. Today* **34**, 7–16 (2020).

66. S. Massa, M. A. Sakr, J. Seo, P. Bandaru, A. Arneri, S. Bersini, E. Zare-Eelanjegh, E. Jalilian, B.-H. Cha, S. Antona, A. Enrico, Y. Gao, S. Hassan, J. P. Acevedo, M. R. Dokmeci, Y. S. Zhang, A. Khademhosseini, S. R. Shin, Bioprinted 3D vascularized tissue model for drug toxicity analysis. *Biomicrofluidics* **11**, 044109 (2017).

67. D. B. Kolesky, K. A. Homan, M. A. Skylar-Scott, J. A. Lewis, Three-dimensional bioprinting of thick vascularized tissues. *Proc. Natl. Acad. Sci. U.S.A.* **113**, 3179–3184 (2016).

68. D. Wang, W. Chen, Indocyanine green angiography for continuously monitoring blood flow changes and predicting perfusion of deep inferior epigastric perforator flap in rats. *J. Invest. Surg.* **34**, 393–400 (2021).

69. D. Huang, T. Liu, J. Liao, S. Maharjan, X. Xie, M. Pérez, I. Anaya, S. Wang, A. Tirado Mayer, Z. Kang, W. Kong, V. L. Mainardi, C. E. Garciamendez-Mijares, G. García Martínez, M. Moretti, W. Zhang, Z. Gu, A. M. Ghaemmaghami, Y. S. Zhang, Reversed-engineered human alveolar lung-on-a-chip model. *Proc. Natl. Acad. Sci. U.S.A.* **118**, e2016146118 (2021).

70. Q. Gao, Y. He, J.-Z. Fu, A. Liu, L. Ma, Coaxial nozzle-assisted 3D bioprinting with built-in microchannels for nutrients delivery. *Biomaterials* **61**, 203–215 (2015).

71. G. Gao, J. H. Lee, J. Jang, D. H. Lee, J.-S. Kong, B. S. Kim, Y.-J. Choi, W. B. Jang, Y. J. Hong, S.-M. Kwon, D.-W. Cho, Tissue engineered bio-blood-vessels constructed using a tissue-specific bioink and

3D coaxial cell printing technique: A novel therapy for ischemic disease. *Adv. Funct. Mater.* **27**, 1700798 (2017).

72. G. Gao, H. Kim, B. S. Kim, J. S. Kong, J. Y. Lee, B. W. Park, S. Chae, J. Kim, K. Ban, J. Jang, H.-J. Park, D.-W. Cho, Tissue-engineering of vascular grafts containing endothelium and smooth-muscle using triple-coaxial cell printing. *Appl. Phys. Rev.* **6**, 041402 (2019).

73. S. C. Millik, A. M. Dostie, D. G. Karis, P. T. Smith, M. McKenna, N. Chan, C. D. Curtis, E. Nance, A. B. Theberge, A. Nelson, 3D printed coaxial nozzles for the extrusion of hydrogel tubes toward modeling vascular endothelium. *Biofabrication* **11**, 045009 (2019).

74. L. Shao, Q. Gao, C. Xie, J. Fu, M. Xiang, Y. He, Directly coaxial 3D bioprinting of large-scale vascularized tissue constructs. *Biofabrication* **12**, 035014 (2020).